Optical Conductivity of Amorphous Ta and β-Ta Films

J.E. Nestell, Jr., K.J. Scoles, and R.W. Christy
Department of Physics and Astronomy, Dartmouth College
Hanover, New Hampshire 03755

Thin films of tantalum evaporated in high vacuum onto fused silica substrates at liquid-nitrogen temperature are amorphous, even after heating above room temperature. On room-temperature substrates β-Ta, with a 30-atom tetragonal unit cell, is deposited. The electron-diffraction interference function of the amorphous a-Ta agreed best with dense-random-packing models, although a β-Ta microcrystalline model also gave fairly good agreement. The complex optical conductivity was determined from reflection and transmission measurements in the spectral range 0.5 - 6.5 eV, at room temperature. The results for a-Ta and β-Ta were very similar to each other, differing significantly from bcc α-Ta (deposited onto heated substrates or crystallized from amorphous films), and they could be extrapolated to the measured dc conductivity at zero energy. After subtraction of a Drude contribution with an electron mean free path on the order of the interatomic distance, the remainder showed some features of the interband absorption in α-Ta, though somewhat smoothed and weakened. We conclude that local disorder of near neighbors is more important than whether long range order exists.

I. INTRODUCTION

In the course of measuring the optical constants of bcc transition metals,[1-3] it was observed that tantalum films evaporated in high vacuum onto liquid-nitrogen-cooled substrates had an amorphous structure that persisted even after warming to room temperature. The optical conductivity (as well as the dc conductivity) of the amorphous films differed significantly from that of the bcc films. Since Ta seems to be exceptional as a relatively pure metal that can exist in an amorphous phase above low temperatures, it offers an unusual opportunity to study an amorphous transition metal over an extended temperature range, with the possibility of separating experimentally the consequences of configurational disorder from those of compositional disorder. In the well known stable metallic glasses, for example, physical effects of topological disorder must be inferred in an alloy of two or more atomic species.

Although the amorphous Ta films were relatively pure, they were undoubtedly stabilized by gaseous impurities accidentally present. From the evaporation rate and background pressure, however, we can estimate that the impurity content (for example, of nitrogen) was less that 1%, an amount that is too small to account for the optical effects to be described below. These conclusions are in accord with other studies of amorphous Ta alloy films[4] and Ta films evaporated in ultrahigh vacuum and doped with nitrogen.[5]

It was also found[1] that Ta films evaporated onto room-temperature substrates had the β-Ta crystal structure. This structure is well known in sputtered Ta films,[6] which have been extensively studied because of their importance in Ta-film capacitors and resistors; it does not require stabilization by impurities.[7] It has a tetragonal unit cell containing 30 atoms.[8] The optical (and dc) conductivity of β-Ta had a much closer resemblance to amorphous a-Ta than to the ordinary stable bcc α-Ta (evaporated onto hot substrates). Thus it seems that the local atomic arrangement of near neighbors may have a more important influence on these electronic properties than does the existence (or absence) of long range order.

Our primary aim was therefore to investigate the structure of amorphous Ta films and to measure their conductivity, in comparison to the bcc crystalline form. The complex β-Ta crystalline form may provide a kind of intermediate case. The results will be discussed with the intent of clarifying the role of the structure in determining the electron density of states and electron scattering. Our sample preparation methods have been described previously.[3] Briefly, the material was electron-beam evaporated onto fused-silica substrates in high vacuum (5×10^{-7} Torr or 7×10^{-5} Pa) at fast rates (> 30 Å/s). Except for dc resistance, all measurements were made after the samples were removed from the vacuum system.

II. FILM STRUCTURES

X-ray diffraction observations were made on the optical samples using a General Electric XRD-5 diffractometer with a copper-target tube, 0.2° slit aperature, and angle calibration against quartz. For the tantalum films transmission electron diffraction (TED) and transmission electron microscopy (TEM) specimens were simultaneously deposited onto the (100) face of Harshaw NaCl or KCl crystals, freshly cleaved (in air). The TED and TEM pictures[9] were made with a Philips 212 electron microscope operated at 80 kV, a Siemens 101 microscope at 80 kV, or a JEOL 100C microscope at 100 kV, on specimens of thickness < 400 Å, stripped from the NaCl or KCl substrates. The TED pictures were scanned with a Joyce-Loebl IIB microdensitometer, using a mechanical magnification of the pattern of 5x, to determine interference functions. The microscope camera length was calibrated using line positions from well-crystallized Ta films.

X-ray diffraction analysis of a 2000-Å thick room-temperature-deposited Ta film showed the β-Ta (002) diffraction line and a low hump composed of unresolved (202) and (330) lines (d = 2.35 and 2.40 Å).[8] Since this spacing also corresponds to the (110) line in the bcc phase (2.34 Å), we cannot rule out the presence of some bcc Ta in this film. The hump was not visible, however, in a thin film (253 Å), which, therefore, must have been pure β-phase since the bcc phase preferentially forms with (110) planes parallel to the substrate[10] and would have been easily detectable. The absence of the hump also indicates a definite preferred β-phase orientation with (001) planes parallel

to the substrate in a thin film (but less in a thicker one). The line position of the (002) reflection for both films gave a lattice constant along the tetragonal c-axis of 5.258 Å, about 1% less than the value for chemically precipitated β-phase material[8] recognized by the ASTM, probably because of tensile stresses in the plane of the film coupled with Poisson's ratio. The line width of the x-ray (002) reflection suggested a grain size of about 120 Å perpendicular to the substrate, according to the Scherrer equation,[11] even though its application to such large unit cells in small grains may be questionable.[12] Electron microscopy (TEM) of the 253-Å β-Ta film showed a grain size in the plane of the film of only about 60Å. The picture showed a reasonably equi-axed grain structure with lighter-colored (lower density) grain boundaries about 5 Å wide, and a few scattered light-colored channels about 100 Å wide, which are possibly an oxide or nitride. The grain boundaries and channels appeared to extend completely through the film, indicative of a columnar microstructure. The TED pattern for this film showed a fine-grained β structure with a split first ring. The first ring is composed of the unresolved low-index lines from the (002) to (411) lines, which all lie close together. The splitting could be explained if some, e.g., the (202) line, were missing or weak.

For the thin Ta films evaporated onto 77-K substrates, x-ray diffraction showed no observable lines, indicating a high degree of disorder. The TED pattern showed three diffuse rings, suggestive of an amorphous phase that will be discussed in more

detail below. TEM photomicrographs showed a rather featureless microstructure (to be expected of an amorphous material) with a granular appearance on the scale of regions 5-10 Å across, which is consistent with dense-random-packing-of-hard-sphere models of amorphous solids[13,14] and does not suggest any sort of microcrystalline structure. On a larger scale there was a faint network of lighter colored boundaries of size and shape similar to the grain boundaries seen in the β-Ta sample. It seems that the film was somewhat inhomogeneous with a columnar microstructure and a network of less dense material between columns. Such a structure is common in amorphous transition metal films.[15,16]

Detailed studies of the diffuse TED pattern for the amorphous Ta film were made in order to elucidate the local atomic arrangement in this highly disordered phase. The ultimate object of such studies is generally to obtain the radial distribution function $\rho(r)$ characterizing the amorphous solid; however, we shall discuss only its more directly observable Fourier transform, expressed in terms of the interference function (or structure factor)[17,18]

$$I(k) = 1 + \int [\rho(r) - \rho_o] \frac{\sin kr}{kr} 4\pi r^2 dr,$$

where ρ_o is the average number density of the irradiated material. The interference function is related to the coherent scattered intensity from N atoms, $N|f(k)|^2 I(k)$, where $f(k)$ is the atomic scattering factor. Thus $I(k)$ can be determined from the observed TED pattern, after making corrections for incoherent scattering and multiple scattering that $I(k)$ does not account for. The experimental electron interference pattern was recorded as density variations in the photographic negative, with film density converted to electron intensity by the method of Karle and Karle.[19] Incoherent and multiple scattering contributions to the measured interference function were estimated and removed, by assuming[20] that they are the same as the baseline in the crystalline state of Ta measured from a crystalline film with the same thickness. The function $|f(k)|^2$ is tabulated in the literature.[21] The resulting interference function, shown in Fig. 1, has a narrow, intense first maximum and broad higher

maxima. (Minor structure in the pattern, especially near the fourth maximum, is due to experimental noise and should be disregarded.)

Models of amorphous solids are of two types: those that assume the atoms are arranged in well defined microcrystals whose extremely small size precludes long range order (and escapes experimental resolution), and those which assume that the atoms are arranged in a liquid-like random packing of near neighbors. Difficulties in distinguishing experimentally between these models are severe.[21,22] Microcrystalline models for amorphous structures are attractive because Bragg peaks of the crystalline structure often align approximately with measured amorphous diffraction maxima,[18] and the Bragg peaks are broadened into diffuse halos when the grain size is extremely small. An approach to deciding whether a particular microcrystalline model adequately describes the lack of long range order is to calculate the interference function from the Debye equation

$$I(k) = \frac{1}{n} \sum_{i \neq j}^{n} \sum^{n} \sin(kr_{ij})/kr_{ij}$$

for scattering from randomly oriented small crystals of n atoms each; r_{ij} is the distance between atoms i and j within a crystallite.[17] Thermal displacements of the atoms can be accounted for by a Debye-Waller damping factor $\exp(-\langle u \rangle^2 k^2)$ and an added background term $1-\exp(-\langle u \rangle^2 k^2)$; we chose a value of 0.001 for $\langle u \rangle^2$ in the model calculation. Since model I(k)

curves have previously been made for pure amorphous Fe and Ni without success,[23] based on the bcc structure for the microcrystals, we calculated the model diffraction for the amorphous Ta pattern based on the more complicated β-Ta tetragonal structure.[8] This crystal structure is not completely understood and two models were considered: the 30 atom/unit cell P4mnm and P4nm structures of β uranium.[24] The results for eight-cell crystallites are shown in Fig. 1. In no case was the microcrystalline model able to reproduce the narrow and intense first maximum of the experimental interference function: If enough cells are added to the crystallites to do so, the subsequent maxima become too sharp and intense. The separation between the second and third maxima in the P4mnm structure is greater than that observed experimentally, but the P4nm curve agrees fairly well with the positions of the second and third maxima. Neither curve reproduces the shape of the fourth maximum at all well.

Another approach to modelling the atomic arrangement in amorphous solids is based on structures formed by the dense random packing of hard spheres (DRPHS). Such structures are dense in the sense that they contain no voids large enough to accomodate another sphere and are random in the sense that there are no strong correlations between the positions of spheres separated by more than a few diameters.[18] In Fig. 2 is shown our experimental interference function for amorphous Ta compared to a DRPHS interference curve.[25] The similarity is evident, although the DRPHS first maximum, like the microcrystalline

models, is too low and broad. This discrepancy, however, can be explained: Only 500 spheres were included in this DRPHS calculation,[25] whereas the intensity and narrowness of the first maximum in DRPHS models increases[26,27] with increasing model size, with no asymptotic behavior yet at 1000 spheres. In addition, the DRPHS model was unrelaxed, in the sense that no local rearrangement of atoms was allowed to minimize the energy of the cluster based on a Lennard-Jones or other soft potential; relaxation also gives a noticeable sharpening of the first peak.[28] Thus we conclude that the DRPHS model can reproduce the observed interference function much better than the microcrystalline model of the amorphous Ta film, even when this is based on a complex (β-Ta) unit cell. The microcrystalline model seems to be incapable of predicting a sufficiently narrow main peak together with broad higher peaks.

III. OPTICAL CONDUCTIVITY

The method of obtaining the optical constants and film thickness from reflectance and transmittance measurements has been described previously.[2,3] These measurements were made on films in the thickness range 250 - 400 Å.

The optical conductivity (in cgs units) of the amorphous tantalum is shown in Fig. 3 as a function of photon energy. For comparison we also show previous results[3] for crystalline bcc α-Ta films. The principal difference is that the amorphous results are much flatter at low energy, with the higher-energy structure somewhat attenuated. The real part σ_1 extrapolates to about 4×10^{15} s^{-1} at $\omega = 0$, in approximate agreement with the measured dc resistivity of the amorphous films; 4×10^{15} s^{-1} = $1/225$ $(\mu\Omega cm)^{-1}$. The real susceptibility is $\chi_1 = -\sigma_2/\omega$.

Results are also shown in Fig. 3 for β-Ta films, and they show a remarkable similarity to the amorphous results, in contrast to the bcc structure. Again the extrapolation of σ_1 to $\omega = 0$ agrees approximately with the measured dc conductivity. It appears that the crystalline structure with a large unit cell resembles the amorphous structure more closely than the simple bcc crystal.

The optical behavior of the amorphous Ta at low energy is suggestive of the Drude free electron formula with a short electron lifetime τ. The Drude result is

$$\frac{\sigma_o}{1 - i\omega\tau} = \frac{\sigma_o}{1 + (\omega\tau)^2} + i\,\frac{\sigma_o\omega\tau}{1 + (\omega\tau)^2} = \sigma_1 + i\sigma_2 ,$$

where the dc conductivity is $\sigma_o = \omega_p^2\tau/4\pi$, with the plasma frequency $\omega_p = (4\pi ne^2/m^*)^{1/2}$. The formula gives a maximum of σ_2 at $\omega\tau = 1$, where $\sigma_2 = \sigma_1 = \frac{1}{2}\sigma_o$. In Fig. 4 are plotted the Drude curves assuming $\sigma_o = 4 \times 10^{15}\ s^{-1}$ and $\tau/\hbar = \frac{1}{2}\ (eV)^{-1}$, or $\tau = 0.33 \times 10^{-15}$ s. These are a good representation of the experimental curves below about 1 eV (assuming a smooth extrapolation to the dc values). If the average Fermi velocity $\overline{v_F}$ is around 1×10^8 cm/s, the mean free path would be $\lambda = \overline{v_F}\tau \approx 3$ Å. The plasma frequency is $\omega_p = 8.1$ eV. Somewhat similar values would also serve for the β-Ta data, whereas the bcc film would have a much longer lifetime.

The dashed curves in Fig. 4 show the difference between the experimental amorphous-Ta curves and the assumed Drude contribution. These may be compared to the dashed curves in Fig. 3, which, above about 2 eV at least, represent the interband contribution in bcc crystalline Ta. The corresponding bound-electron part of the amorphous conductivity is clearly important: although the Drude lifetime could be somewhat shorter than assumed, the mean free path λ could not be less than about 3 Å within the context of the Drude theory, and so the bound-electron part has to be significant. More precisely, if the free-electron result is assumed also for the Fermi velocity, $v_F = \hbar(3\pi^2 n)^{1/3}/m^*$, one finds $\lambda = \hbar(3\pi^2/n^2)^{1/3}\ \sigma_o/e^2$ for a given σ_o, independent of the assumed τ. Then the effective number of electrons per atom

must be less than about 1.5. Consequently, if we also assume $m^* \geq m$, there is a limit $\tau > 0.2 \times 10^{-15}$ s or $\tau/\hbar > \frac{1}{4}$ $(eV)^{-1}$. A shorter τ could not make any sense in a free-electron theory (with the given σ_o).

The crystalline bcc Ta data (Fig. 3) also show a clear suggestion of free-electron behavior below about 1 eV. Although an accurate fit to the Drude formula has not been achieved for Ta even in the infrared,[29] we can make a rough estimate of the electron lifetime as in the amorphous case. Using $\sigma_o = 29 \times 10^{15}$ s^{-1} measured[5] on thin films, we find that $\tau = 3.8 \times 10^{-15}$ s ($\tau/\hbar = 5.8$ eV^{-1}) leaves an interband contribution which tends properly to zero with ω. (The corresponding plasma frequency would be $\omega_p = 6.4$ eV.) Thus we conclude that the free-electron lifetime and mean free path are an order of magnitude less in amorphous Ta or β-Ta than in α-Ta films.

It is more difficult to make a quantitative comparison of the bound-electron contributions with the α-Ta case, because of the possible effects of the fine grains in β-Ta and of the faint network in a-Ta that were observed in the TEM pictures. Pronounced grain boundaries on this scale have been shown[2] to affect the optical conductivity of the Cr-group metals with bcc grains. Therefore we applied the same inhomogeneous-medium model to hypothetical small grains of bcc Ta, to see whether the effective conductivity could simulate the observed results for a-Ta and β-Ta. The outcome was that it could, if some 25% of the total volume were in the boundary network and the conductivity of the boundary material were only about 5% of the grain interior (in

the notation of Ref. 2, c = 0.06, c' = 0, k = 0.06). Thus, if the inhomogeneity of the β-Ta and a-Ta films were this severe, the intrinsic conductivity of homogeneous material with these structures could actually be identical to that of the bcc crystal. Since, however, the inhomogeneity of the β-Ta and a-Ta films in fact appeared less severe, on the TEM evidence, we conclude that the differences in bound-electron conductivity are probably real structure effects, at least in part. In any case, the grain boundaries would not affect the free-electron lifetime drastically, since the mean free path is already much less than the grain size.

IV. DISCUSSION

We now want to compare the α-, β-, and a-Ta phases with respect to their atomic structure and electronic conductivity, with the hope of identifying relationships between these properties. The structure has to be discussed on three increasing distance scales: i) the local configuration of near neighbors of a given atom; ii) long range crystalline order (periodicity); and iii) grain boundaries or similar microscopic inhomogeneities. The observed conductivity was separated into i) a free-electron contribution that is consistent with the dc resistivity; and ii) the interband part, or an analogous bound-electron remainder in a-Ta.

The diffraction measurements on α- and β-Ta films showed the accepted crystalline structure, but possibly with about 1% homogeneous strain in β-Ta. This kind of homogeneous strain has been found not to affect the optical reflectivity in other metals.[3] The diffuse diffraction rings from the a-Ta films were analyzed in some detail in an effort to distinguish between the microcrystalline and random-packing models for the local atomic arrangement. We based our microcrystalline modelling on the 30-atom β-Ta unit cell, since earlier attempts based on the bcc cell have generally failed. The results actually gave a fairly good correspondence with the observed amorphous interference function— much better than those based on the bcc cell— suggesting the primary importance of the near-neighbor arrangements. Still, the minimal amount of long range order in this model (8 unit cells) excessively emphasized the higher interference peaks in comparison to the first one, which was too broad. Thus

we found that the random-packing model could give a better account of our a-Ta film structure, in general agreement with previous work on amorphous metal films and metallic glasses. In the absence of small-angle-scattering measurements, the diffraction gave no information about microscopic inhomogeneities or grain boundaries, except through broadening of the Bragg diffraction peaks in β-Ta. A more direct picture came from the electron microscopy of β- and a-Ta, which showed a boundary network on the scale of 50 to 100 Å, but could not give much information about the atomic structure of the boundary material.

The optical conductivity was fitted at lower photon energies with the Drude formula so as to agree with the dc resistivity. The resulting electron lifetime (scattering rate) corresponded to a mean free path only just greater than the interatomic distance in β- and a-Ta, less than the unit-cell size of β-Ta. In α-Ta, on the other hand, the lifetime was an order of magnitude larger. The remainder (the interband part in α- and β-Ta) was also very similar in β- and a-Ta, with peaks around 3 eV and 5 eV that were somewhat attenuated in comparison to α-Ta.

The free-electron lifetime of the amorphous material should depend on the structure factor associated with the Fourier transform of the potential seen by the conduction electrons.[30] This theory can account for the high dc resistivity of amorphous metals, including its temperature dependence at least in some cases.[31] Although the structure factor for 100-keV electrons would not have to be the same, still the similarity that was noted (Fig. 1) between the amorphous and the β-Ta microcrystalline structure factors might be expected to remain at all electron

energies. This could not by itself account for the similar lifetimes in β-Ta and a-Ta, however, since the observed grain size in the β-Ta films was large enough to give the delta-function type structure-factor peaks that result in Bragg diffraction and band gaps at the zone boundaries in crystals. Thus the much shorter lifetime in β-Ta, as compared to α-Ta, is presumed to depend on the complex unit cell of β-Ta. The effect of the 30-atom unit cell on the band picture would be to split every bcc energy level (at a given $\underline{k}$) into 30 levels (some of which might be degenerate); the qualitative result would be a proliferation of branches crossing the Fermi level and fragmentation of the Fermi surface. This might increase large-angle electron scattering near the Fermi surface by offering many more possibilities for umklapp scattering, and thus shorten the mean free path in β-Ta. Once the mean free path is shorter than the unit cell dimension, long range order can have no more effect, so that the near equality of the β-Ta and a-Ta lifetimes could then actually stem from the similarity of the structure factors.

There is no way that <u>all</u> of the observed conductivity of a-Ta could be due to free-electron behavior; i.e., there is certainly an appreciable contribution corresponding to the interband absorption in α-Ta. The latter has been attributed[3] to transitions between d bands— the main peak at 5 eV due principally to band 3 → 5, and the feature at 3 eV to 3 → 4 transitions. From the standpoint of a tight binding approximation to the d-band states, these states might indeed be expected to survive in the amorphous phase, a relatively narrow d band being

more characteristic of the individual atom than of the long range order. In fact, however, although these features do survive in a-Ta, they appear to be somewhat weaker than in α-Ta. This effect may depend primarily on the matrix elements of the transitions: In the free atom d-to-d transitions are forbidden, and their prominence in the crystal is explained by hybridization of the d bands with s-p bands; presumably the absence of symmetry in a-Ta reduces the amount of s-p mixing, and therefore decreases the matrix elements. The situation in β-Ta could be similar to a-Ta, since with 30 atoms in the unit cell the local symmetry of near neighbors is reduced. (In the bcc structure, a 27-atom cluster would include the third-shell neighbors.) Very similar effects have been observed[32] in α-Mn, another transition metal with a large (29-atom) unit cell.

These considerations are also consistent with earlier observations on liquid metals.[33] For Fe, Co, and Ni, the absorption of the liquid in the 2-3-eV range is about the same as for the crystal,[34] where it is probably due mainly to the 3 → 5 d-band transitions in these 3d metals. Since the liquid would have an appreciable free-electron contribution there as well, judging from its measured dc conductivity, the d-to-d band absorption is somewhat attenuated compared to the crystal, just as in a-Ta. In Cu, the liquid absorption is also about the same as in the crystal, but the free-electron contribution is smaller. In the Cu crystal,[35] the absorption is mainly from the band 5 → 6 transitions; this has a d-to-p character, which is allowed even in the free atom, so less attenuation might be expected in the liquid. In liquid Al, on the other hand, the parallel-band nearly-free-electron transition at 1.5 eV in the crystal is

wiped out completely. Similar behavior was observed[36] in amorphous films of Ga and Bi, where the crystalline peaks are also supposed to arise from transitions between nearly-free-electron states.

Apparently no theoretical calculations of optical conductivity have yet been attempted for an amorphous transition metal, although there are recent calculations of the d-band density of states.[37,38] These were based on atom positions generated by DRPHS models, and so in this respect they should be applicable to our amorphous Ta films (Fig. 2). The energies were calculated in the tight-binding approximation with only nearest-neighbor overlap; the overlap integrals were given values appropriate for nickel[37] and cobalt,[38] but qualitatively the results should still be useful in discussing tantalum. Generally the density-of-states function seems to have two main peaks and to be smoother than the crystalline density of states, with a shape that is governed by the first maximum of the radial distribution function, i.e., by the local distribution of near neighbors. The smoothness is probably responsible for the washing out of some features of the optical conductivity of a-Ta (and also β-Ta) as compared to α-Ta. Unfortunately these results have limited further applicability to the optical problem, since no mixing of the d states with s-p states was included in the calculation; we argued above that hybridization seems to have a major effect on the transition matrix elements.

Some additional insight may be had from calculations for crystalline transition metals. Again, no optical conductivity calculations are available for Ta, although a self-consistent APW calculation[39] has included a breakdown of the s-, p-, and

d-band densities of states. Optical calculations for V and Nb (as well as Cr and Mo) show reasonable agreement with experiment, as discussed in Ref. 3, with regularities that can probably be extrapolated to the case of Ta. A basic difference between the amorphous and the crystalline states is that $\underset{\sim}{k}$ is not a good quantum number in the amorphous structure; thus the idea of a "nondirect" transition of the crystal may have some bearing: A nondirect optical transition is defined as one in which k-conservation is not an important selection rule. Although nondirect transitions are not presently thought to be important in crystals, they have been treated theoretically, and a comparison of direct and nondirect calculations for Mo showed a great similarity.[40] This is not surprising,[41] since the transitions are mostly between rather flat d bands which are not strongly dependent on $\underset{\sim}{k}$ anyway, so that in either case the optical peaks depend on the joint density of states. Therefore the mere lack of the k quantum number is probably not a very significant consequence of the disorder in transition metals. On the other hand the band-to-band matrix elements are quite dependent on $\underset{\sim}{k}$ in crystals, as a consequence of angular momentum selection rules; thus calculations that assume constant matrix elements have not given good agreement with experiment: For example, a constant-matrix-element calculation[42] for V (and Cr) showed a large optical peak due to band 2 → 5 transitions because these bands are very flat near the symmetry line D (between N and P) in the zone face. Inclusion of calculated matrix elements[43,44] suppressed the 2 → 5 transitions, probably because both bands are largely d-like[39] and transitions are forbidden by the dipole

selection rule. We concluded above that such considerations are also (or even more) important in the amorphous phase.

To summarize, we found that the structural disorder in amorphous Ta films, which is well described by a DRPHS model, affects both intraband and interband optical conductivity. A Drude part that is consistent with the dc resistivity arises from a shortened mean free path, of the order of the interatomic distance. The remaining absorption shows some of the features of the bcc crystal, but smeared out and weakened. The similarity of the results in β-Ta suggests the primary importance of the local arrangement of near neighbors rather than the existence of long range order. Some smearing can be expected from theoretical density-of-states calculations with local disorder. The transition probabilities are unlikely to be much affected by the lack of the k-conservation selection rule, but the angular momentum selection rule retains its importance. Thus a realistic theoretical calculation of the optical properties would have to include d-band hybridization with s-p bands and calculated matrix elements. These conclusions would seem to extend to other amorphous transition metals as well.

This work was supported by NASA.

REFERENCES

1. J.E. Nestell, Jr., Ph.D. thesis, Dartmouth College, 1978 (unpublished). See also K.J. Scoles, Ph.D. thesis, Dartmouth College, 1982 (unpublished).
2. J.E. Nestell, Jr., R.W. Christy, Mitchell H. Cohen, and G.C. Ruben, J. Appl. Phys. 51, 655 (1980).
3. J.E. Nestell, Jr., and R.W. Christy, Phys. Rev. B 21, 3173 (1980).
4. M.M. Collver and R.H. Hammond, J. Appl. Phys. 49, 2420 (1978).
5. A. Schafer and G. Menzel, Thin Solid Films 52, 11 (1978).
6. M.H. Read and C. Altman, Appl. Phys. Lett. 7, 51 (1965).
7. A. Schafer and G. Menzel, Electrocomponent Sci. Technol. 4, 29 (1977).
8. P.T. Moseley and C.J. Seabrook, Acta. Cryst. B29, 1170 (1973).
9. The electron microscopy was done by Dr. G.C. Ruben.
10. M.H. Read and D.H. Hensler, Thin Solid Films 10, 123 (1972).
11. H.P. Klug and L.E. Alexander, X-Ray Diffraction Procedures for Polycrystalline and Amorphous Materials (Wiley, New York, 1974), p. 687.
12. Sir W.H. Bragg and W.L. Bragg, eds., The Crystalline State, V.2. "The Optical Principles of the Diffraction of X-rays" by R.W. James (G. Bell, London, 1933), Ch. 10.
13. J.F. Graczyk and P. Chaudhari, Phys. Stat. Solidi B 75, 593 (1976).
14. R. Alben, G.S. Cargill, III, and J. Wenzel, Phys. Rev. B 13, 835 (1976).
15. P. Chaudhari and D. Turnbull, Science 199, 11 (1978).
16. A.G. Dirks and H.J. Leamy, Thin Solid Films 47, 219 (1977).

17. A. Guinier, X-Ray Diffraction (Freeman, San Francisco, 1963), Ch. 2 and 3.
18. G.S. Cargill, III, Solid State Physics, Vol. 30 (Academic Press, New York, 1975) p. 227.
19. J. Karle and I.L. Karle, J. Chem. Phys. 18, 957 (1950).
20. S. Fujime, Jap. Appl. Phys. 5, 764 (1967).
21. G.S. Cargill, III, J. Appl. Phys. 41, 12 (1970).
22. B.G. Bagley, H.S. Chen, and D. Turnbull, Mater. Res. Bull. 3, 159 (1968).
23. T. Ichikawa, Phys. Stat. Solidi. (a) 19, 707 (1973).
24. Ralph W.G. Wyckoff, Crystal Structures, 2nd Ed., V. 1 (Interscience, New York, 1963), p. 44.
25. G.S. Cargill, III, AIP Conf. Proc. No. 31 (AIP, New York, 1976), p. 339.
26. J.F. Sadoc, J. Dixmier, and A. Guinier, J. Non-Crys. Solids 12, 46 (1973).
27. J.G. Wright, Inst. Phys. Conf. Ser. 30, 251 (1977).
28. G.S. Cargill, private communication.
29. M.M. Kirillova, L.V. Nomerovannaya, and M.M. Noskov, Sov. Phys. Solid State 16, 1425 (1975).
30. J.M. Ziman, Models of Disorder (Cambridge, 1979), Chap. 10.
31. S.R. Nagel, Phys. Rev. B 16, 1694 (1977).
32. K.J. Scoles and R.W. Christy, Phys. Rev. B, to be published.
33. J.C. Miller, Phil. Mag. 20, 1115 (1969).
34. P.B. Johnson and R.W. Christy, Phys. Rev. B 9, 5056 (1974).
35. P.B. Johnson and R.W. Christy, Phys. Rev. B 11, 1315 (1975).
36. O. Hunderi, Thin Solid Films 37, 275 (1976).

37. S.N. Khanna and F. Cyrot-Lackmann, Phil. Mag. B 38, 197 (1978).

38. S.N. Khanna and F. Cyrot-Lackmann, Phys. Rev. B 21, 1412 (1980).

39. L.L Boyer, D.A. Papaconstantopoulos, and B.M. Klein, Phys. Rev. B 15, 3685 (1977).

40. D.D. Koelling, F.M. Mueller, and B.W. Veal, Phys. Rev. B 10, 1290 (1974).

41. W.E. Pickett and P.B. Allen, Phys. Rev. B 11, 3599 (1975).

42. G.V. Ganin, M.M. Kirillova, L.V. Nomerovannaya, and V.P. Shirokovskii, Fiz. Met. Metalloved. 43, 907 (1977).

43. V.L. Moruzzi, A.R. Williams, and J.F. Janak, private communication to P.B. Johnson and R.W. Christy described in Ref. 34.

44. D.G. Laurent, C.S. Wang, and J. Callaway, Phys. Rev. B 17, 455 (1978).

FIGURE CAPTIONS

Fig. 1 Interference function of amorphous Ta as a function of $k = 4\pi \sin\Theta/\lambda$. Curve A: experimental result; curve B: calculated for microcrystals consisting of 8 unit cells (240 atoms) of β-Ta structure, P4mnm symmetry; curve C: same as B, P4nm symmetry.

Fig. 2. Interference function of amorphous Ta. Curve A: experimental result; curve B: calculated from DRPHS model (Ref.25). The hard-sphere radius is a.

Fig. 3. Optical conductivity, $\sigma_1 + i\sigma_2$, of amorphous Ta (heavy line) and β-Ta (light line), in comparison to bcc α-Ta (dashed line) from Ref. 3.

Fig. 4. Optical conductivity according to the Drude theory with dc conductivity $\sigma_o = 4 \times 10^{15}\ s^{-1}$ and electron lifetime $\tau = 0.33 \times 10^{-15}$ s (solid curves). The dashed curves show the difference between the experimental data for amorphous Ta (heavy curves in Fig. 3) and the Drude curves.

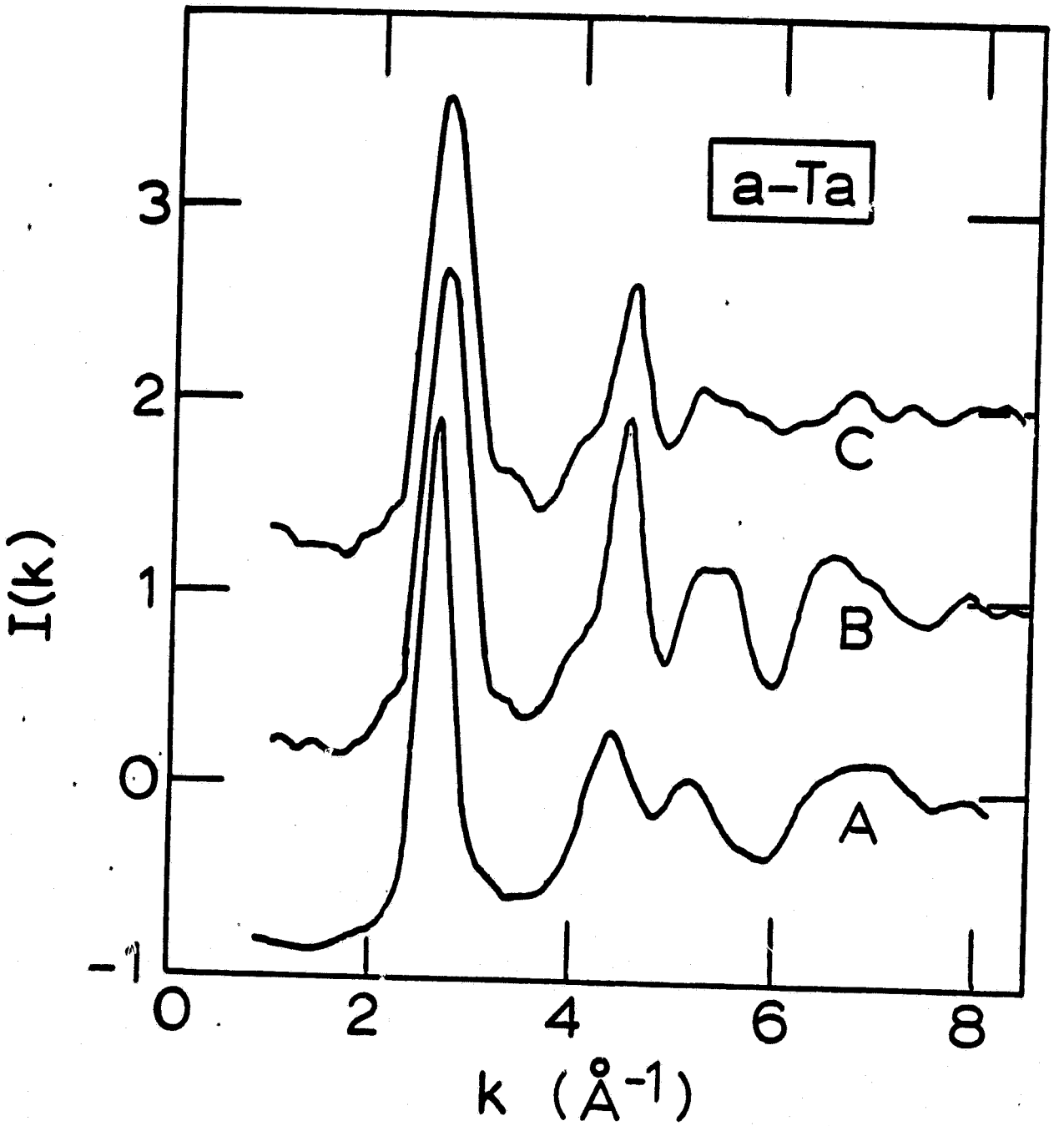

Fig. 1

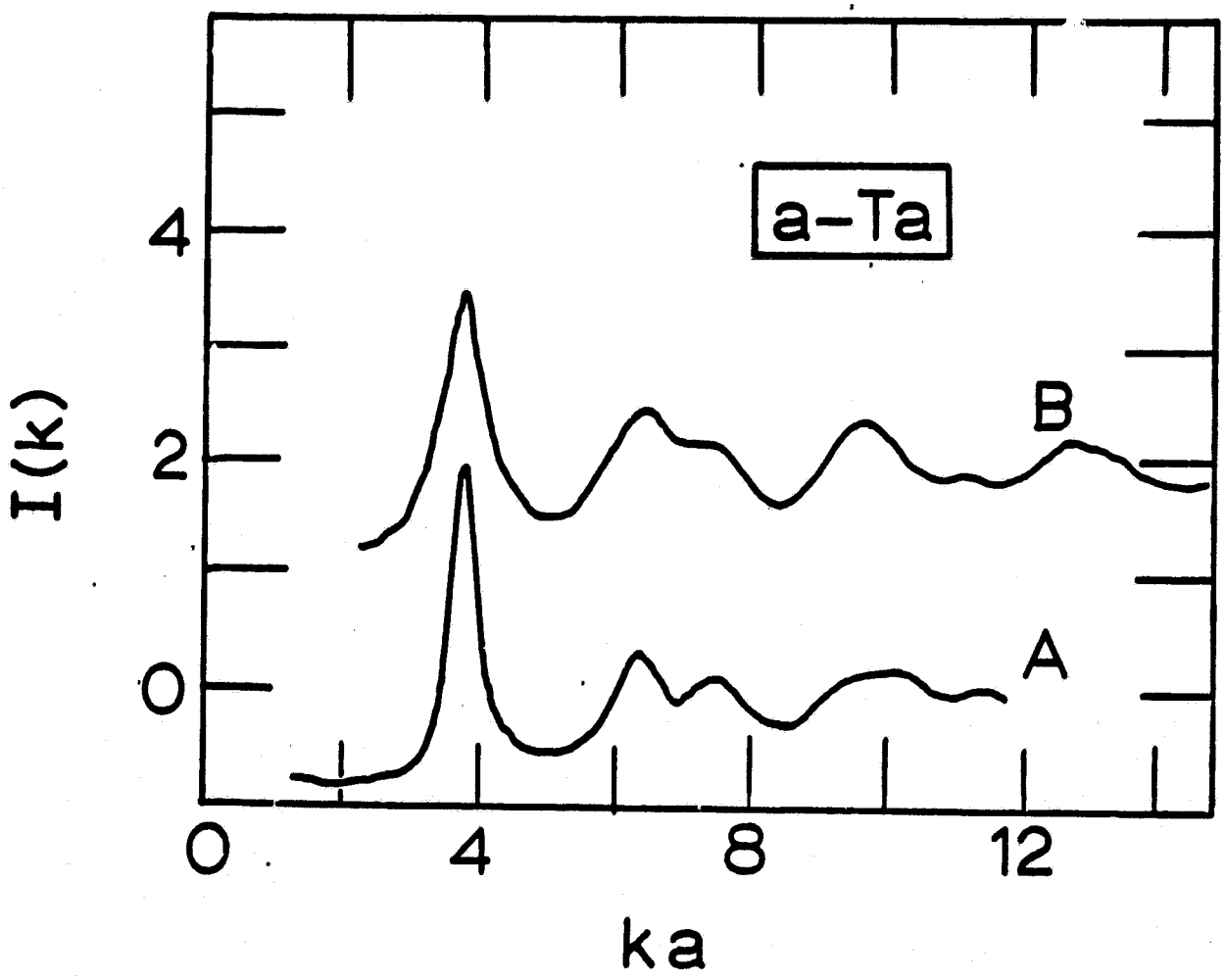

Fig. 2

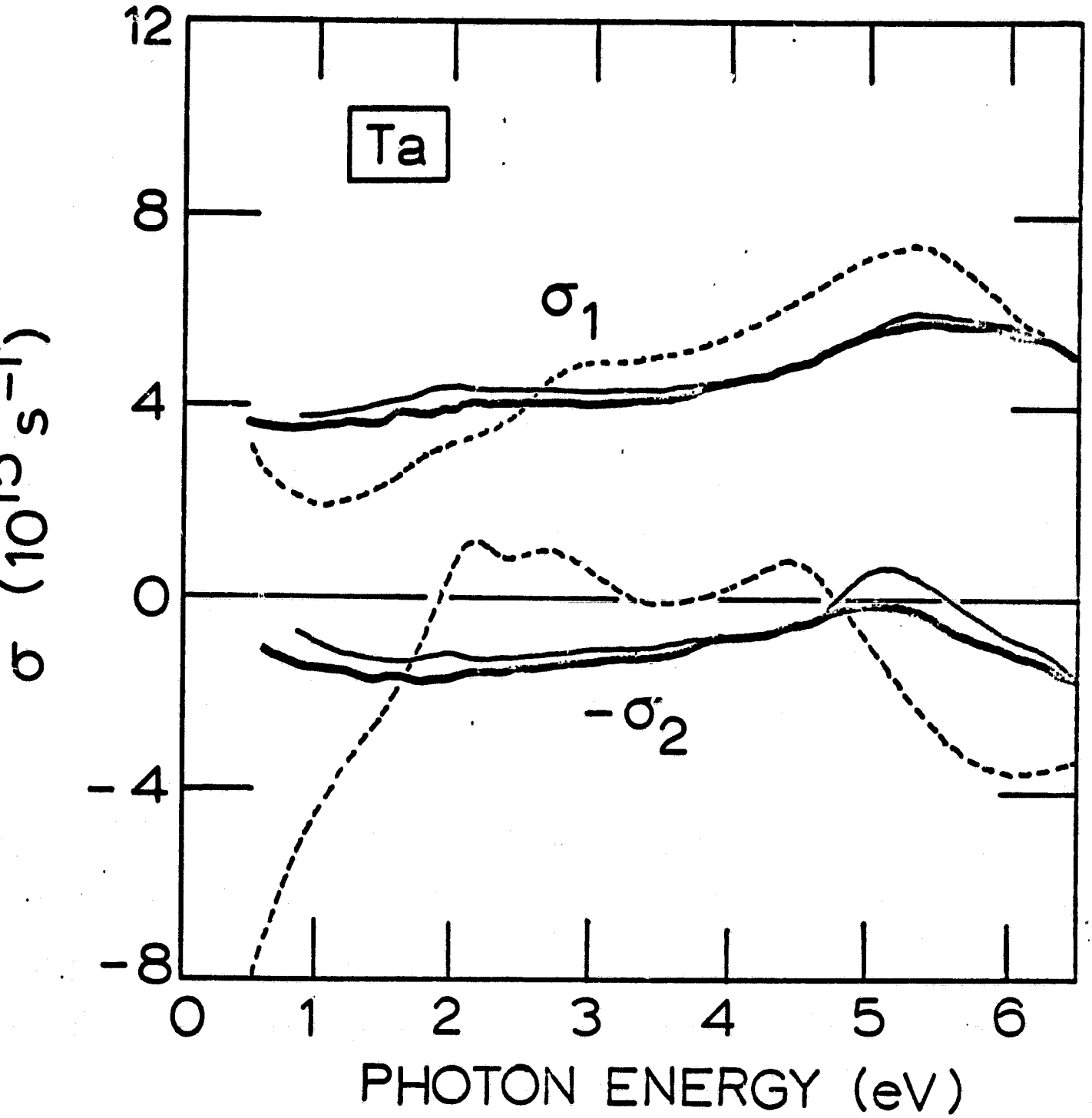

Fig. 3

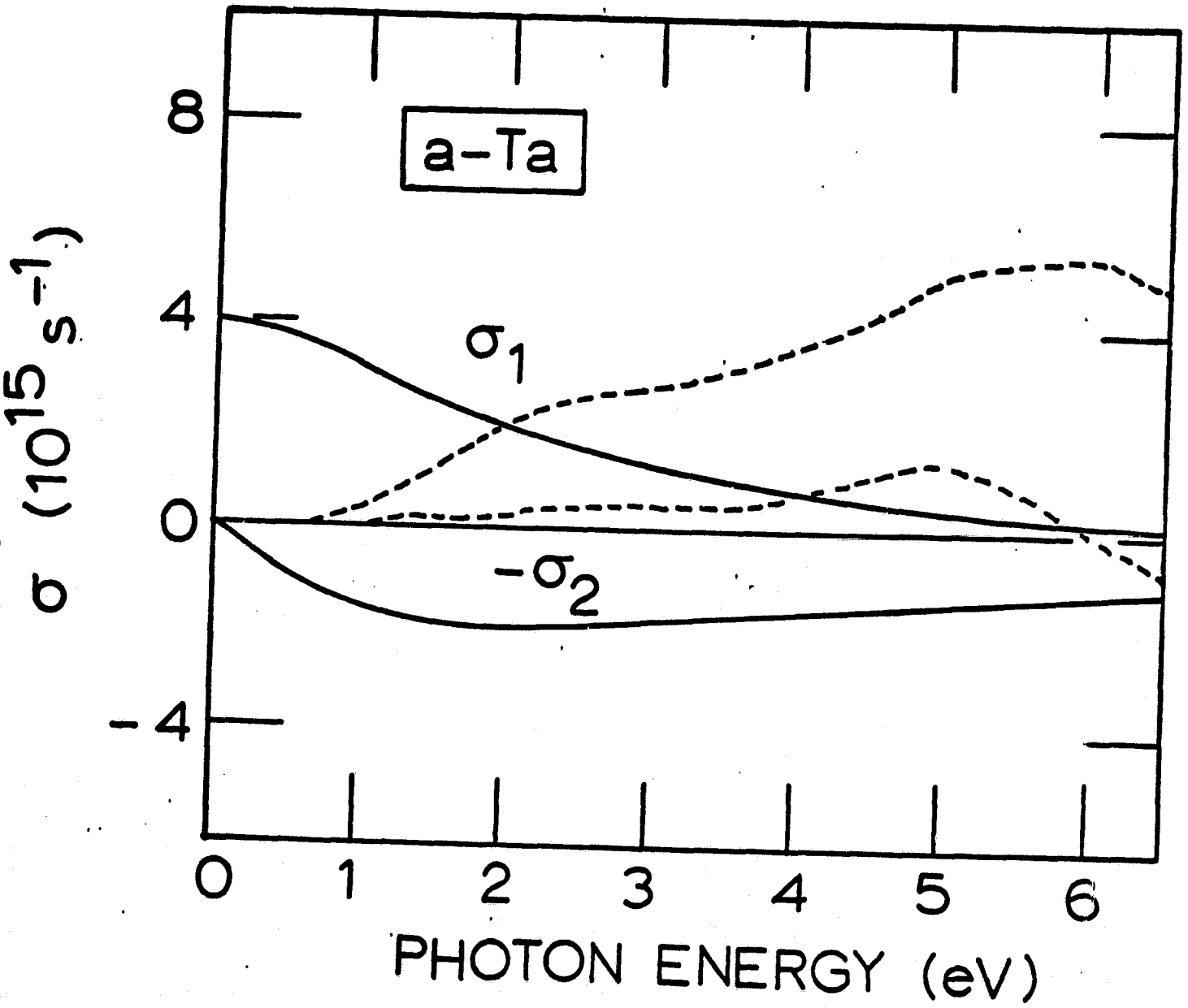

Fig. 4